

# Ab-initio simulation of photoinduced transformation of small rings in amorphous silica

Davide Donadio

*Computational Science, Department of Chemistry and Applied Biosciences,  
ETH Zurich USI Campus, Via Giuseppe Buffi 13, CH-6900 Lugano, Switzerland*

Marco Bernasconi

*Dipartimento di Scienza dei Materiali and INFN,  
Università di Milano-Bicocca, via Cozzi 53, I-20125 Milano, Italy*

We have studied the photoinduced transformation of small rings (3-membered) in amorphous silica by Car-Parrinello simulations. The process of ring opening leading to the formation of a couple of paramagnetic centers, namely an  $E'$  and a non-bridging-oxygen hole center (NBOHC), has been proposed experimentally to occur in silica exposed to  $F_2$  laser irradiation (at 7.9 eV). By using a new scheme for the simulation of rare events in ab-initio molecular dynamics (Iannuzzi, Laio and Parrinello, Phys. Rev. Lett. **90**, 238303 (2003)), we have identified the transformation path for the opening of a 3-membered ring induced by a self-trapped triplet exciton, the migration of NBOHC and formation of a couple of stable  $E'$  and NBOHC paramagnetic defects.

PACS numbers: 61.43.Fs; 61.72.Ji; 71.23.-k; 71.15.Pd

Extensive experimental and theoretical studies have been devoted to point defects in amorphous silica due to their relevance in the degradation of  $SiO_2$ -based electronic devices and in the photosensitivity of optical fibers [1]. For instance, it is well established that the possibility to change the refractive index and write Bragg gratings in optical fibers by UV illumination is connected to the photoinduced transformation of pre-existing defects or the formation of new ones. The formation of defects in amorphous silica upon  $F_2$  excimer laser irradiation is also held responsible for the degradation of lenses for optical lithography in semiconductor technology [2].

In a recent experimental work Hosono *et al.* [2] proposed that the main channel for color center formation in silica exposed to radiation of an  $F_2$  excimer laser (7.9 eV, well below the Tauc band gap of a- $SiO_2$ ) is the generation of an  $E'$  center and a non-bridging-oxygen hole center (NBOHC) from one-photon excitation and breaking of strained bonds in small (3- or 4-membered) rings. The experimental evidence comes from combined Electron Paramagnetic Resonance (EPR), Raman and optical spectroscopy measurements which show a correlation between the intensities of the Raman lines associated to the breathing modes of 3- and 4-membered rings ( $D_1$  and  $D_2$  lines) in samples with different fixation temperatures and the appearance of EPR and optical absorption signals assigned to  $E'$  and NBOHC radicals. From these correlations Hosono *et al.* inferred that one-photon absorption processes at  $\sim 7.9$  eV generate excitons self-trapped on the small rings which would lead to ring opening and pair formation of  $E'$  and NBOHC defects as shown in Fig. 1.

In this paper we report the results of ab-initio simulations of the photoinduced processes leading to the opening of small rings in a- $SiO_2$  aiming at providing theoretical support to the mechanism of  $E'$ -NBOHC pair genera-

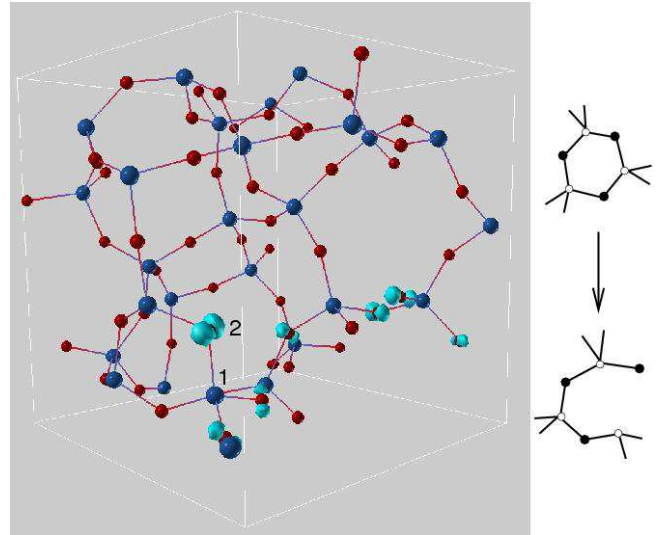


FIG. 1: Left panel: electron density of the hole of the triplet exciton self-trapped on a 3-membered ring in a 81-atoms model of a- $SiO_2$ . The contour value on the electron density plot is 0.125 a.u.. The Kohn-Sham orbital is mostly localized on the oxygen atom O(2). Right panel: path for the pair generation of the  $E'$  and NBOHC radicals upon photoexcitation of a 3-membered ring as proposed in Ref. [2].

tion proposed experimentally. The main outcome of the simulation is that the configuration of the two paramagnetic centers proposed experimentally and shown in Fig. 1 is metastable on the excited state, but the ring spontaneously closes once the system is brought back on the electronic ground state. However, a stable  $E'$ -NBOHC pair is found via a further migration of the NBOHC.

Ab-initio Car-Parrinello [3, 4, 5] molecular dynamics (MD) simulations have been performed within the frame-

work of density functional theory in the local spin density approximation supplemented by generalized gradient corrections [6, 7]. Norm conserving pseudopotentials [8], plane wave expansion of Kohn-Sham (KS) orbitals up to a kinetic energy cutoff of 70 Ry, a fictitious electronic mass of 800 a.u. and a time step of 0.15 fs have been used. The photoinduced transformations have been simulated by adiabatic Born-Oppenheimer MD on the lowest triplet ( $T_1$ ) excited state energy surface. Although the photoinduced reaction would occur on the singlet excited state, MD on the  $T_1$  excited energy surface is more easily affordable within our framework and would provide transformation paths that also shed light on the processes induced by the singlet excitons as we have already demonstrated in a previous work on the photoinduced interconversion of oxygen deficient centers in a-SiO<sub>2</sub> [9].

Periodic models of a-SiO<sub>2</sub> containing 81 atoms at the experimental density of 2.2 g/cm<sup>3</sup> have been generated by quenching from the melt in classical MD, adopting the empirical pair potential by van Beest *et al.* [10]. Quenching times as long as 5 ns have been used in the classical simulations in order to generate models with a small number of 3- and 4-membered rings. Three models have been generated, one with one 3- and four 4-membered rings, a second with one 3- and five 4-membered rings, and a third one with no 3- and one 4-membered ring. The classical models have been then annealed at 600 K for 1.5 ps by ab-initio MD. This procedure has been already demonstrated to provide models of a-SiO<sub>2</sub> with good structural, elastic and dielectric properties [11, 12, 13]. By exciting the system on the lowest triplet state, we have found that for the first among the models considered the hole of the exciton is partially localized on the 3-membered ring. The self-trapped triplet exciton is shown in Fig. 1. Hereafter all the simulations presented would refer to this latter model. The triplet exciton induces a slight lengthening of the Si(1)-O(2) bond in Fig. 1 by 0.03 Å, but the ring is still locally stable. The transformation leading to the opening of the ring turns out to be an activated process with an energy barrier much larger than the thermal energy. Thus it would not occur spontaneously on the time scale of Car-Parrinello simulations, few tens of ps long. In order to overcome this limitation, we have exploited a new technique [14] recently devised to simulate rare events within Car-Parrinello MD. The method is based on a coarse-grained dynamics in the space of few reaction coordinates, biased by a history-dependent potential which drives the system toward the lowest transition state [14, 15, 16]. The total energy of the locally stable configurations and transition states found along the transformation path have been then refined by constrained geometry optimization [18]. The activation energies of the different processes have been then estimated, although in principle also the entropic contributions to the activation free energies could be computed within the method of Ref. [14]. Due to the relatively large size of

our simulation cell and the long simulation time needed to get accurate free energy estimates, we have restricted ourselves to the calculation of activation energies and not free energies. Entropic effects are small anyway for the breaking of siloxane bonds at room temperature as shown in Ref. [19].

Following the scheme of Ref. [14], the collective reaction coordinates  $S_\alpha(\{\mathbf{R}_I\})$ , function of the ionic positions  $\mathbf{R}_I$ , define a set of associated collective variables  $s_\alpha$  which are treated as new dynamical variables. The extended system is described by the Lagrangian

$$L = L_o + \sum_{\alpha} \frac{1}{2} M_{\alpha} \dot{s}_{\alpha}^2 - \sum_{\alpha} \frac{1}{2} k_{\alpha} (S_{\alpha}(\{\mathbf{R}_I\}) - s_{\alpha})^2 (1) \\ - V(t, \{s_{\alpha}\}),$$

where  $L_o$  is the Car-Parrinello Lagrangian, the second term is the fictitious kinetic energy of the  $s_{\alpha}$ 's, the third term is a harmonic potential that restrains the value of the collective coordinates  $S_{\alpha}(\{\mathbf{R}_I\})$  to the corresponding dynamic collective variables  $s_{\alpha}$ .  $V(t, \{s_{\alpha}\})$  is the Gaussian-like history dependent potential defined in ref. [14].

In a first simulation, we have used a single collective variable which provides a measure of the length of the Si(1)-O(1) bond (cfr. Fig. 1) which is lengthened upon excitation on the triplet state. Namely, we have chosen the coordination number  $n_{Si(1)-O(2)}$  between atoms Si(1) and O(2). Following Ref. [14], the coordination number between atom  $a$  and atoms  $b$  is defined as  $n_a = \sum_b \frac{1 - (\frac{r_{ab}}{d})^6}{1 - (\frac{r_{ab}}{d})^{14}}$  where  $r_{ab}$  is the distance between the two atoms and scaling factor  $d$  is chosen as  $d=2.2$  Å.  $n_a$  estimates the number of atoms  $b$  within the bond cut-off distance to atom  $a$  and decays smoothly for larger distances. Recent investigations have shown that the best efficiency of the method would be achieved in our case when the collective variable has a characteristic frequency ( $\sqrt{k/M}$ ) of the same order of magnitude as the Si-O stretching mode [17]. Accordingly, we have chosen  $M=1.82 \cdot 10^5$  a.u. and  $k=1$  a.u. in Eq. (1) ( $\sqrt{k/M} \sim 10^{14}$  s<sup>-1</sup>). The parameters which define the history-dependent Gaussian potential in Eq. (3) of Ref. [14] are  $\delta s^{-1} = 0.08$  and  $W = 0.002$  Hartree. MD simulations have been performed at 300 K [20].

Under the effect of the driving history-dependent potential the ring opens in 4.5 ps leading to the configuration reported in Fig. 2b. Its energy, obtained by geometry optimization, is -0.27 eV with respect to the energy of the closed ring on the  $T_1$  excited state which is chosen hereafter as our zero of energy. At this point the electron of the triplet exciton is self-trapped on Si(1). In the configuration of Fig. 2b two paramagnetic defects are formed (an E' center on Si(1) and a NBOHC on O(2), 3 Å far apart) by breaking the Si(1)-O(2) siloxane bond and overcoming an activation barrier of 0.38

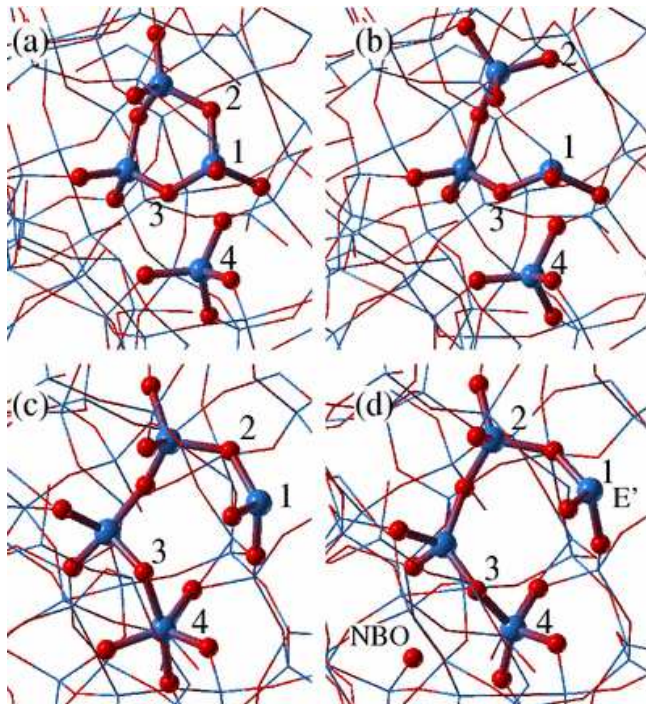


FIG. 2: Snapshots of the locally stable configurations found along the path that leads to the formation of an E'-NBOHC pair from the photoinduced opening of a 3-membered ring. The atoms involved in the transformation are represented by spheres and connected by thicker sticks. (a) The 3-membered ring excited on the  $T_1$  state. (b) The adjacent E'-NBOHC defect pair. (c) The E' center and the 5-coordinated silicon atom. (d) The stable E'-NBOHC pair.

eV. The energy barrier is obtained from constrained ab-initio MD simulations [18] at different values of a reaction coordinate chosen as the Si(1)-Si(2) distance. The configuration in Fig. 2b is locally stable on the  $T_1$  excited state, but by de-exciting the system on the ground state ( $S_0$ ), we have observed a charge transfer from the E' center to the NBOHC which leads to a spontaneous closure of the ring [21]. Therefore, the two paramagnetic defects in the configuration of Fig. 2b are not stable in the ground state and cannot be assigned to the EPR signals observed experimentally. We may envisage to stabilize the E'-NBOHC pair by reducing the interaction between the two radicals to be realized by allowing a migration of one of two paramagnetic centers. In order to identify this process we have added a second collective variable in Eq. (1), defined as the coordination number  $n_{Si(1)-O(3)}$  between atoms Si(1) and O(3) in Fig. 2a. The presence of both the  $n_{Si(1)-O(2)}$  and  $n_{Si(1)-O(3)}$  collective variables allows to explore different paths for the ring opening. The parameters  $M$ ,  $k$ ,  $\delta s^\perp$  and  $W$  are the same as before. In this second simulation the system initially follows the same path seen in the previous one which means

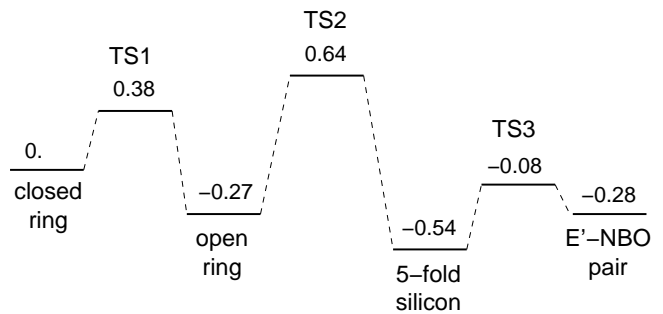


FIG. 3: Energies of the optimized local minima corresponding to the configurations of Fig. 2. Closed ring, open ring, 5-fold silicon and E'-NBOHC pair refer to panels a, b, c and d of Fig. 2, respectively. The energy and geometry of the transition states TS1, TS2 and TS3 are obtained from constrained geometry optimization [18] by using as reaction coordinate respectively the distance Si(1)-O(2), Si(1)-O(3) or Si(4)-NBO in Fig. 2.

that the Si(1)-O(2) bond is weaker than the Si(1)-O(3) one. However, as the simulation proceeds, the history-dependent potential drives the system away from the local minimum of Fig. 2b. First, the Si(1)-O(2) bond is recovered and then a new conformation of the open ring is formed by breaking the Si(1)-O(3) bond. The NBOHC generated in this way (on O(3)) floats around and finally forms a new bond with Si(4) which becomes 5-fold coordinated. This process has a higher activation barrier (0.64 eV) but leads to a configuration (Fig. 2c) which is locally stable with a total energy of -0.54 eV. From this configuration it is now envisageable to generate a new NBOHC by breaking one of the five Si(4)-O bonds. To identify which Si(4)-O bond is most prone to break, we have started a third simulation from the configuration of Fig. 2c with the total coordination number  $n_{Si(4)-O}$  as collective variable. The final structure of this latter process is shown in Fig. 2d. Its total energy is -0.28 eV and the activation barrier for the formation of the NBOHC is 0.46 eV (Fig. 3). The E' and the NBOHC centers in this final configuration are distant enough (6.3 Å) to prevent the charge transfer upon de-excitation on the  $S_0$  state. As the two radicals do not interact each other, there is no singlet-triplet splitting and the EPR signals are supposed to be equal to those of the isolated paramagnetic centers. The path identified by the local minima of Figs. 2a-c represents thus a viable mechanism for the opening of the ring and migration of the NBOHC suitable to provide a pair of stable paramagnetic defects. The total trajectory starting from the initial configuration of Fig. 2a and reaching the final configuration of the stable E'-NBOHC pair in Fig. 2d is 2.7 ps long. The energies of the configurations in Fig. 1 and of the transition states separating the different local minima are collected in the scheme of Fig. 3. The geometry of the transition state

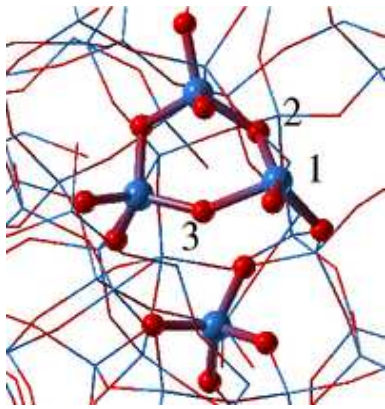


FIG. 4: Geometry of the transition state TS2 of Fig. 3. The distances between the silicon atom Si(1) and the oxygen atoms O(2) and O(3) are 1.80 Å and 2.05 Å, respectively. The tetrahedron formed by atom Si(1) is highly distorted and undergoes a puckering once a NBOHC is formed on O(3) (cfr. Fig. 2c). As a consequence the resulting E' center that does not point towards the NBOHC.

leading to the 5-fold coordinated Si is reported in Fig. 4. We remark that the recovery of the Si(1)-O(2) bond moving from configuration in Fig. 2b to the transition state in Fig. 4 does not restore the initial configuration of the closed ring (Fig. 2a). No intermediate local minima from Fig. 2b to Fig. 2c is found. The activation barrier for the whole process (the energy of the highest transition state) is 0.64 eV, sufficiently low to make this transformation channel viable at room temperature. These values for the activation energies are supposed to depend on the local environment and strain of the small ring. As a consequence only a fraction of the small rings are expected to undergo this transformation upon photoexcitation.

In summary, we have identified the transformation path for the opening of a 3-membered ring induced by a self-trapped triplet exciton. Once open in the excited electronic state, the 3-membered ring gives rise to a couple of strongly interacting E' and NBOHC defects, which recombine quickly after electronic de-excitation. However, a simple path with a low energy barrier (0.64 eV) has been identified for the migration of the NBOHC which leads to the formation of a couple of stable E' and NBOHC paramagnetic centers. The simulations thus provide a theoretical support to the interpretation of the experimental data in Ref. [2] on the formation of color centers in a-SiO<sub>2</sub> by F<sub>2</sub> laser irradiation.

We gratefully thank M. Iannuzzi, A. Laio and M. Parrinello for discussion and for sharing with us their insight on the new methods they have developed. D.D. acknowledges financial support from Pirelli Cavi e Sistemi S.p.a. This work is partially supported by the INFM Parallel Computing Initiative.

\*corresponding author: ddonadio@phys.chem.ethz.ch

- 
- [1] *Defects in SiO<sub>2</sub> and Related Dielectrics: Science and Technology*, Edited by G. Pacchioni, L. Skuja, and D. L. Griscom, NATO Science Series (Kluwer Academic Publisher, Dordrecht, 2000).
  - [2] H. Hosono *et al.*, Phys. Rev. Lett. **87**, 175501 (2001).
  - [3] R. Car and M. Parrinello, Phys. Rev. Lett. **55**, 2471 (1985).
  - [4] CPMD V3.7, Copyright IBM Corp 1990-2003, Copyright MPI fuer Festkoerperforschung Stuttgart 1997-2001.
  - [5] D. Marx and J. Hutter in *Modern Methods and Algorithms of Quantum Chemistry*, Forschungszentrum Juelich, NIC Series, Vol. 1 (2000) p.301.
  - [6] A. D. Becke, Phys. Rev. **A 38**, 3098 (1988).
  - [7] C. Lee, W. Yang, and R. G. Parr, Phys. Rev. **B 37**, 785 (1988).
  - [8] N. Troullier and J.L. Martins, Phys. Rev. **B 43**, 1993 (1991).
  - [9] D. Donadio, M. Bernasconi and M. Boero, Phys. Rev. Lett. **87**, 195504 (2001).
  - [10] B. W. H. van Beest *et al.*, Phys. Rev. Lett. **64**, 1955 (1990).
  - [11] D. Donadio, M. Bernasconi, and F. Tassone, Phys. Rev. **B 68**, 134202 (2003).
  - [12] M. Benoit, S. Ispas, P. Jund, and R. Jullien, Eur. Phys. **J. B 13**, 631 (2000).
  - [13] J. Sarthain, A. Pasquarello and R. Car, Phys. Rev. **B 52**, 12690 (1995).
  - [14] M. Iannuzzi, A. Laio and M. Parrinello, Phys. Rev. Lett. **90**, 238302 (2003).
  - [15] A. Laio and M. Parrinello, Proc. Nat. Acad. Sci. **99**, 12562 (2002).
  - [16] C. Micheletti, A. Laio and M. Parrinello, Phys. Rev. Lett., **92**, 170601 (2004).
  - [17] A. Laio, private communication.
  - [18] M. Sprik and G. Ciccotti, J. Chem. Phys. **109**, 7737 (1998).
  - [19] M. Boero, A. Oshiyama, and P.L. Silvestrelli, Phys. Rev. Lett. **91**, 206401 (2003).
  - [20] Constant temperature is enforced by velocity rescaling at the target temperature with a tolerance of 10 %.
  - [21] We have performed additional calculations on cluster model by using the B3LYP [7, 22] functional in order to check the effect of the functional on the E' → NBOHC charge transfer mechanism identified in the simulation. In fact, the BLYP functional is expected to underestimate the Hubbard-U parameter on the oxygen radical due to incomplete correction of the self-interaction. On the contrary the self-interaction is exactly cancelled within the B3LYP functional. We have considered two clusters ·Si(OSiH<sub>3</sub>)<sub>3</sub> and ·O(SiH<sub>3</sub>) at different Si-Si distances. We have found that the charge transfer occurs for E'-NBOHC distances below 5 Å for the B3LYP functional and below 5.4 Å for the BLYP functional. The calculations have been performed with the code Gaussian98 [23] and the 6-311+G\* basis set which provides a good description of point defects in silica [24].
  - [22] A. D. Becke, J. Chem. Phys. **98**, 5648 (1993).
  - [23] GAUSSIAN98, M. J. Frisch, G. W. Trucks, H. B. Schlegel *et al.* (Gaussian Inc., Pittsburgh, Pennsylvania 1998).
  - [24] G. Pacchioni and M. Vitiello, J. non-Crystall. Solids, **245**, 175 (1999).